Penerbit Akademia Baru

Journal of Research in Nanoscience and Nanotechnology

Journal homepage:
http://akademiabaru.com/submit/index.php/jrnn/index
ISSN: 2773-6180

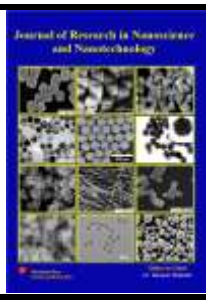

Green Synthesis of *Guaiacum officinale* L. Leaf Extract Silver Nanoparticles for Potential Antioxidant and Anticancer Activity

Purohit Rangavitala[1], Tarikere Chandrashekharappa Taranath[1,*]

[1] Environmental Biology and Green Nanotechnology Laboratory, P. G. Department of Studies in Botany, Karnatak University, Dharwad – 580003, Karnataka, India
* Correspondence: tctaranath@gmail.com
https://doi.org/10.37934/jrnn.12.1.2540

ABSTRACT

The green synthesis of AgNPs using ultrasonic-assisted hydroacetonic *Guaiacum officinale* L. leaf extract (GoLE), which contains phytochemicals, can play a substantial role in bio-reduction, capping, and stabilization of the nanoparticles. The colour change was observed from light yellow to brown indicating the synthesis of *Guaiacum officinale* leaf extract silver nanoparticles (GoLE-AgNPs). The absorption maxima (λ_{max}) of AgNPs at 411 nm were confirmed by UV-vis spectroscopy. FTIR data revealed the functional groups involved in the reduction and capping of AgNPs. Powder XRD and SAED images confirmed crystallinity. HR-TEM images showed spherical, ~18-25 nm sized nanoparticles and EDS spotted the strong peak of silver at 3 KeV. DLS spectra results the surface zeta potential of stable nanoparticles at -37.3 mV, +35.4 nm particle size in hydrodynamic solution. Polyphenolic content of GoLE-AgNPs was demonstrated by TPC and TFC. Dose-dependent radical scavenging activity of AgNPs was performed by the DPPH method. GoLE-AgNPs were treated with human bone marrow neuroblastoma (SH-SY5Y) cancer cells at 12.5-200 µg/mL concentration. The effective cell viability of 24.05 ± 0.029% was observed using an MTT assay. GoLE-AgNPs induced 66.13% of apoptosis in cancer cells. Present research results revealed the better antioxidant and anticancer activity of AgNPs.

Keywords:

Anticancer, Antioxidant, *Guaiacum officinale* L., Hydroacetonic extract, Silver nanoparticles, Ultrasonic-assisted extraction

Received: 20 Mar. 2024	Revised: 15 Apr. 2024	Accepted: 18 May. 2024	Published: 30 Jun. 2024

1. Introduction

The characteristic materials in the range of 1–100 nm known as nanoparticles differ noticeably from those of the same material in bulk. These variations in the physicochemical and biological properties and surface-to-volume ratio of nanoparticles bring up a wide range of research opportunities and potential applications [1]. Ultrasonic-assisted extraction (UAE) method and

hydroacetonic solvent facilitated the rapid and effective extraction technique using ultrasound to generate fast movement of solvents, resulting in high acceleration of extraction and higher mass transfer speed [2]. The physical and chemical synthesis of nanoparticles was toxic to the environment, technically challenging, and more expensive. Hence, the eco-friendly, easy-to-synthesize, and less expensive green synthesis method utilizes plant extracts for the synthesis of metal nanoparticles [3]. Silver nanoparticles are more important than other metal nanoparticles because of their diverse applications in antimicrobial, anti-inflammatory, antioxidant, and anticancer drugs in biomedical research [4-7].

Guaiacum officinale L., well known as Lignum vitae (family: Zygophyllaceae). Leaf, bark, and flower of *Guaiacum officinale* are rich sources of saponins such as guaiazulene or guaiac were widely used for antibacterial, antiseptic, and anti-inflammatory [8], antirheumatic and antioxidant [9], anti-tumor and epithelizing properties [10].

Furthermore, the toxic impact of conventional treatment creates radiation, chemotherapeutics, and drug-resistance properties generating an immediate need for the advancement of unconventional treatment for cancer. Additionally, the most esoteric and deadly form of pediatric cancer that develops in the neurological system of young children and offspring and a solid carcinogenic tumor that starts to grow in the nerve cells outside the brain is known as human bone marrow neuroblastoma [11].

The literature study recommends the existence of rich medicinal properties and previously, the synthesis of nanoparticles from *Guaiacum officinale* plants was not reported. Hence, the present investigation was designed for the green synthesis of AgNPs from ultrasound-assisted hydroacetonic leaf extract, characterized the synthesized GoLE-AgNPs, and focused on the potential invitro evaluation of antioxidant and anticancer efficacy of AgNPs against human bone marrow neuroblastoma cancer (SH-SY5Y) cell lines.

2. Materials and Methods

2.1. *Materials*

Milli-Q water was used for the preparation of solutions, 70% Acetone, Folin-Ciocalteu reagent, Aluminum chloride ($AlCl_3$), 2,2-diphenyl-1-picrylhydrazyl (DPPH), Silver Nitrate ($AgNO_3$), 3-(4,5-dimethylthiazol-2-yl)-2,5-diphenyl tetrazolium bromide (MTT), Dimethyl sulfoxide (DMSO) and other reagents, chemicals and stains were obtained from distinguished companies.

2.2. Collection and Authentication

Fresh green leaves of *Guaiacum officinale* L. were collected from Railway quarters, near the Gadag Railway station; 15°26'01.3"N 75°38'32.2"E; Vidya Nagar, Kalasapur, Gadag-Betageri; GPS co-ordinates of the plant: 15.43389, 75.64232; Plus Code: CJMR+FWM Gadag-Betageri, Karnataka, India-582101; Altitude: 654 m/2,146 ft. The collected specimen was critically inspected for morphological characteristics along with the concerned literature. For future reference, a prepared herbarium was kept in the P. G. Department of Botany lab, Karnataka Science College, Dharwad, Karnataka, India-580001 (accession number: Bot/KSCD/28-06-2022/19608).

2.3. Preparation of Plant Extract and Synthesis of GoLE-AgNPs

Collected leaves of *Guaiacum officinale* were washed with tap water and then Milli-Q water to remove all impurities and shade-dried for a week. Thoroughly pulverized to form fine powder. UAE

was performed using Athena Multifunctional Ultrasonicator Cleaner bath model (ATS-10L), Ultrasonic power of 240 W, heating power of 500 W, and frequency of 40 KHz applying direct sonication method developed by Liu *et al.,* [12], Pandhari and Taranath [13], and standardized as per the requirements. 50 grams of pulverized leaf powder with 400 mL of 70% acetone (1:8 w/w) in a 1 L autoclavable bottle stoppered with air condenser, 75 min of extraction maceration and 100% sonication power with 60 ℃ temperature was maintained. Kept for cooling at room temperature for 3 hrs., vacuum filtered twice with Whatman filter paper (No. 1) (Whatman PLC, Maidstone, UK). The filtered extract was air-dried into pellets. The total percentage yield of UAE extract was calculated using the Eq. (1):

$$\% \text{ Yield} = \frac{\text{Weight of the leaf extract}}{\text{Weight of the plant material}} \times 100 \quad (1)$$

Five grams of hydroacetonic leaf extract was diluted with 50 mL of milli-Q water and used for green synthesis of AgNPs. To reduce silver ions, 10 mL diluted aqueous leaf extract was mixed with 20 mL of 1mM aqueous $AgNO_3$, incubated overnight at 25 ℃, and adjusted to pH 8 by adding 1 N NaOH solution and stirred for 10 min.

2.4. Characterization of GoLE-AgNPs

Synthesized AgNPs were diluted with Milli-Q water in 1:5 ratio and absorption spectra were recorded using a double-beam JASCO UV-VIS NIR V670 spectrophotometer with 300-800 nm wavelength range. The purification of AgNPs was performed using REMI Cooling Centrifuge C24 BL (5000 rpm, 15 min) and washed with Milli-Q water thrice, the supernatant was discarded, and the concentrated slurry (containing AgNPs) was collected and dried at 40 ℃ and preserved for characterization. KBr pellets were prepared with purified AgNPs for the analysis of FTIR spectroscopy using Thermo-Fischer Scientific Nicolet 6700 equipment with 400-4000 cm^{-1} scanning range and a resolution of 4 cm^{-1} was used to determine the phytochemicals involved in the reduction, capping, and stabilization of GoLE-AgNPs. The crystallinity of AgNPs was measured using RIGAKU Smartlab SE X-ray diffractometer equipped with Cu Kβ radiation (λ = 1.3923 Å) with 40 kV, 30 mA power, 2θ range of 5~90° and scanning rate was 10.00°/min. The size and shape of the GoLE-AgNPs were determined by HR-TEM (Thermo-Fisher TALOS F200 G2) combined with SAED and EDS was performed to check the crystalline orientation and elemental composition of AgNPs. The surface charge, hydrodynamic size and polydispersity index (PDI) of GoLE-AgNPs were examined by Dynamic light scattering (DLS) analysis using the HORIBA SZ-100 instrument.

2.5. Determination of Antioxidant Activity of GoLE-AgNPs

2.5.1 Total phenolic content (TPC) and total flavonoid content (TFC)

The Folin-Ciocalteu assay developed by Bankalagi *et al.,* [14] was adopted to quantify the TPC of GoLE-AgNPs. Briefly, to maintain proper concentration, 1 mg of GoLE-AgNPs was dissolved in Methanol (1 mg/mL). In a test tube, 1 mL AgNPs was added to 5 mL of Milli-Q water, and 50% Folin-Ciocalteu reagent (1 mL) was added. After 3 min. 3 mL of saturated 2% Na_2CO_3 solution was added and mixed thoroughly. The mixture was left in the dark for 90 minutes at room temperature. The absorbance of the colour generated was measured at 720 nm. A standard curve of known Gallic acid equivalent values (12.5-200 µg/ml) taken as reference. TFC of GoLE-AgNPs was determined using an $AlCl_3$ colorimetric assay described by Chandra *et al.,* [15] Briefly, 1 mg of GoLE-AgNPs was dissolved

in methanol (1mg/mL) separately. 1 mL of 10% $AlCl_3$ solution, 1 mL of 1M NaOH, and 5 mL of Milli-Q water added to the 0.5 mg of silver nanoparticles and incubated for 30 min. at room temperature. Using Milli-Q water (5 mL), a blank was prepared from the same procedure. Absorbance was measured at 420 nm wavelength by using UV–Visible spectrophotometer. A standard curve of known Quercetin equivalent values (12.5-200 µg/mL) taken as a reference. The XY-linear regression graphs were plotted for TPC and TFC values using GraphPad Prism version 8.0.1 software (GraphPad Software, Boston, MA, USA). The experiments were conducted in triplicates and the results were reported as mean ± standard deviation (SD).

2.5.1. DPPH Radical-Scavenging Activity

The green-synthesized GoLE-AgNPs were tested for antioxidant capacity by the DPPH method described by Reddy *et al.*, [16] The GoLE-AgNPs with different concentrations (12.5, 25, 50, 100, 200 µg/mL) were mixed with 3 mL of methanolic solution containing 0.1 mM DPPH radicals. After proper agitation, allowed to incubate for 30 minutes in the dark. Absorbance was recorded at 517 nm using a UV-Vis Spectrophotometer. Ascorbic acid was used as the standard and experiments were carried out in triplicates. The percentage of free-radical scavenging activity was calculated using Eq. (2):

$$\text{DPPH radical scavenging activity (\%)} = \left(\frac{\text{Absorbance of control} - \text{Absorbance of sample}}{\text{Absorbance of control}}\right) \times 100 \quad (2)$$

2.6. Determination of Anticancer Activity of GoLE-AgNPs

2.6.1. Cell culture conditions and assay controls

SH-SY5Y cell lines were bought from the National Centre for Cell Sciences (NCCS), Pune, India. Cancer cells were preserved in T25 culture flask (#12556009, Biolite-Thermo) containing high glucose DMEM (#AL111, HiMedia) and 10% FBS (#RM10432, Himedia). Incubated in the CO_2 incubator (Heal Force, China) at 37 ℃ temperature humidified atmosphere of 5% CO_2 and sub-cultured every 24 hours. A 96-well plate (Corning, USA) seeded with 200 µl of cell suspension, with 20,000 cells per well. After this, the plate spent a full day at 37 ℃ in an incubator with 5% CO_2 [13]. SH-SY5Y cells were treated with Camptothecin as a positive control. Cells cultured in a medium without experimental drug served as negative control and the test group contained cancer cells treated with different concentrations of GoLE-AgNPs prepared in DMSO (0.1%).

2.6.2. MTT cell viability assay

SH-SY5Y cell lines treated with GoLE-AgNPs and a chemotherapeutic drug Camptothecin (#C9911, Sigma-Aldrich) were used as standard. After 24 hrs. of incubation, the medium was removed, MTT reagent (#4060, HiMedia) (0.5 mg/ml) was added and 100 µl of DMSO (#PHR1309, Sigma-Aldrich) dissolved the MTT formazan crystals and absorbance was measured at 570 nm [17]. Cell viability percentage was calculated using Eq. (3):

$$\text{Cell viability (\%)} = \left(\frac{\text{Mean absorbance of treated cells}}{\text{Mean absorbance of untreated cells}}\right) \times 100 \quad (3)$$

The IC_{50} value was calculated by using a linear regression equation Y=Mx+C.
Where, Y = 50, M and C values were derived from the viability graph.

2.6.3. *Annexin V FITC/PI Apoptotic study*

SH-SY5Y cells were cultured in a 6-well plate at a density of $0.5x10^6$ cells/2 ml. subjected to IC_{50} concentrations of GoLE-AgNPs and Camptothecin. After 24 hrs. of incubation, the medium was removed and cells were rinsed with PBS and added to 200µl of trypsin-EDTA (#TCL099, HiMedia) solution, incubated for 3-4 minutes at 37 °C. Culture medium (2 ml) was added, and cell lines were harvested into 12×75 mm polystyrene tubes and centrifuged at 300 x g at 25 ℃ for 5 minutes. Cells were rinsed in PBS twice [16] and 5µl of Annexin V FITC (#51-65874X, BD-Biosciences) was added, gently vortexed, and incubated in the dark for 15 minutes at room temperature. Each tube was gently vortexed after adding 400µl of 1X binding buffer and 5µl of PI (#51-66211E, BD-Biosciences). Using the fluorescence-activated cell sorting (FACS) method, cells were analyzed as described by Koopman *et al.,* [18].

3. Results and Discussion

3.1. *Total Yield of UAE Crude Extract*

15 g of hydroacetonic crude extract was produced from 50 g of *Guaiacum officinale* L. leaf powder using an ultrasonic-assisted extraction method. The resulting total percentage of yield was 31.66 w/w.

3.2. *Characterization of Silver Nanoparticles*

The formation of silver nanoparticles was observed by colour change from light yellow to brown and the excitation of surface plasmonic resonance (SPR) vibrations of synthesized silver nanoparticles at pH 8 indicating the sharp UV-vis absorption maxima (λ_{max}) at 411 nm (Figure 1) [19].

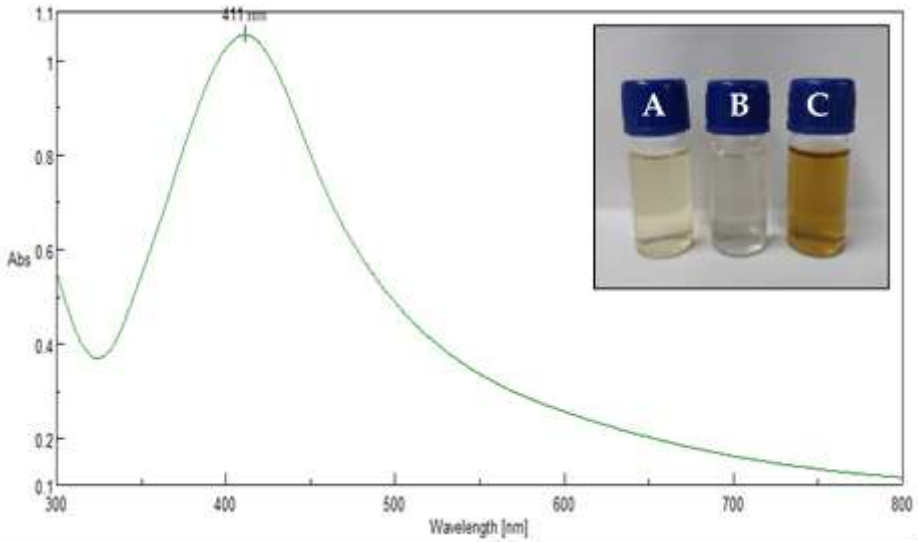

Fig. 1. UV-vis spectrum of GoLE-AgNPs (A) Leaf extract (B) 1mM $AgNO_3$ (C) Reaction mixture

FTIR analysis of GoLE-AgNPs was performed to confirm the phytochemicals reduction and stability of AgNPs. Figure 2 showed the absorbance peak at 3571.57 and 3446.31 cm^{-1} corresponds to the O-H stretching of free alcohol and phenolic compounds serving in the stabilization of AgNPs [20], due to the presence of protein residues the absorbance peak at 1638.92 cm^{-1} represents the C=C medium stretching of cyclic alkenes. The medium stretching absorbance at 1384.27 and 1071.47 cm^{-1}

spectrum corresponds to the C-H stretch of phenols, aldehydes, and alkanes which accelerates the reduction of Ag ions [21,22]. It is evident that the phytochemicals present in the leaf extract act as reducing agents and enhance the AgNPs stability during the synthesis [23].

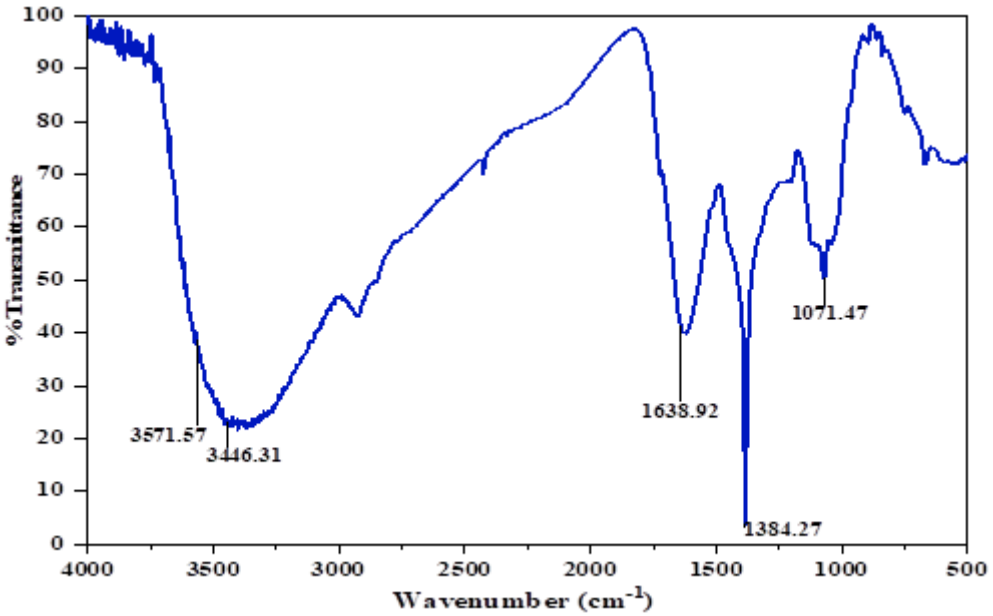

Fig. 2. FTIR spectral analysis of GoLE-AgNPs

The powder X- ray diffractogram of GoLE-AgNPs (Figure 3) showed the miller indices at (111), (200), (220), (311) and (222) which corresponds to Bragg's peaks (2θ angle) at 38.16°, 44.48°, 64.51°, 77.39° and 81.46° which confirms the formation of elemental silver with face centered cubic (FCC) crystalline phase indexed with ICDD Card No. 03-065-2871 and 01-073-6859. Several unassigned peaks which might be due to the crystallization phase of bio-organics that are present on the external surface of the synthesized AgNPs [24]. The average crystalline size of GoLE-AgNPs was calculated using Debye-Scherrer equation, $D = K\lambda/\beta\cos\theta$ where 'D' is the diameter of the nanoparticle, the Scherrer constant K = 0.94 is the shape factor, 'λ' is the wavelength of diffracted X-rays; 'β' represents the full width at half maximum (FWHM) of the peaks and 'θ' is the Bragg's angle, the average size of synthesized AgNPs was found to be 29.85 nm [25].

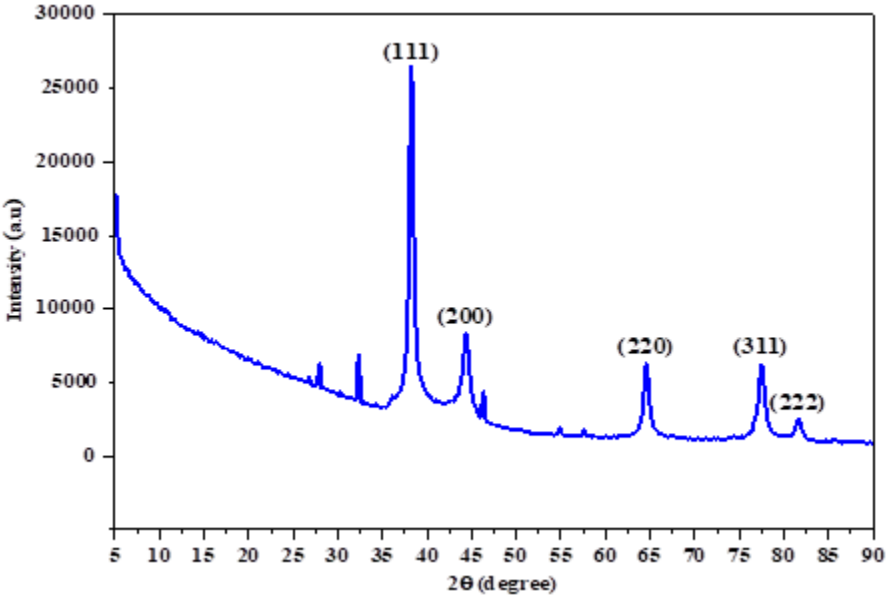

Fig. 3. Powder XRD spectra of GoLE-AgNPs

HR-TEM images (Figure 4A, 4B and 4C) confirm the size of the GoLE-AgNPs, ranging from 18-25 nm in diameter with an average size of ~21.5 nm and spherical-shaped, smooth edges with less agglomeration. The SAED pattern (Figure 4D) of synthesized silver nanoparticles showed a circular diffraction pattern along with bright spots indexed based on the fcc structure of silver. Five bright rings compared to the (111), (200), (220), (311) and (222) lattice planes of fcc silver, which confirmed that the synthesized silver nanoparticles had maintained a regular lattice pattern with good crystallinity and the results were good agreement with XRD data [26]. EDS profile (Figure 4E) confirms the presence of elemental silver at 3 keV and the presence of carbon and oxygen elements in the range of 0.1-0.5 keV because the plant extracts act as capping materials on the nanoparticles' surfaces which are bound to silver nanoparticles surfaces during extraction process [27].

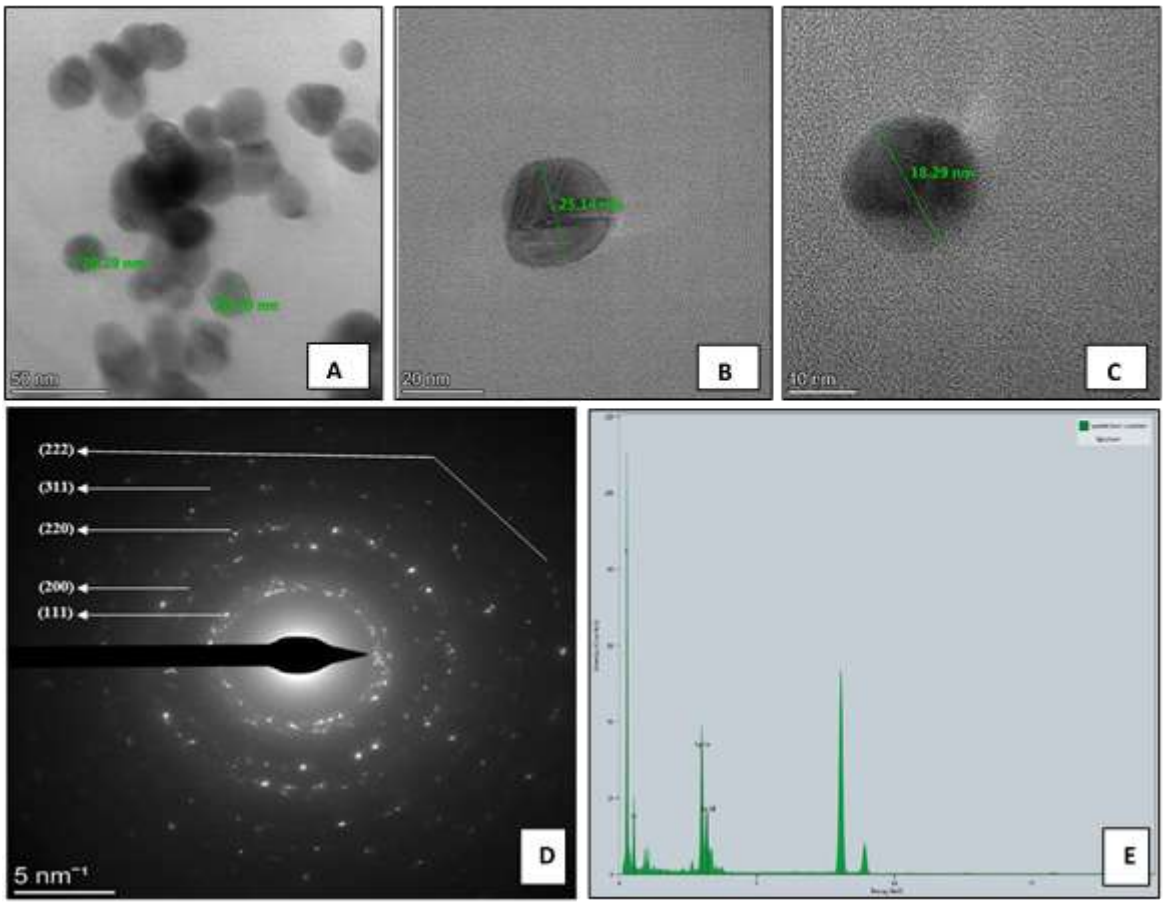

Fig. 4. HR-TEM images of GoLE-AgNPs (A-C) ranging from 18-25 nm along with (E) SAED pattern and (F) EDS spectrum of GoLE-AgNPs

The surface zeta potential of GoLE-AgNPs was found to be -37.3 mV (Figure 5A) indicating the stable anions on the nanoparticles surface which has a strong repulsive force, hence it restricted the aggregation of nanoparticles and enhanced the stability of synthesized nanoparticles. Figure 5B depicts the hydrodynamic size (Z-average size) of synthesized AgNPs was +35.4 nm and the AgNPs were typically distributed in aqueous medium and the measure of the width of the AgNPs size distribution known as polydispersity index (PDI) was found to be 0.600 [28]. The PDI value of AgNPs was less than 1 indicating the monodisperse distribution [29].

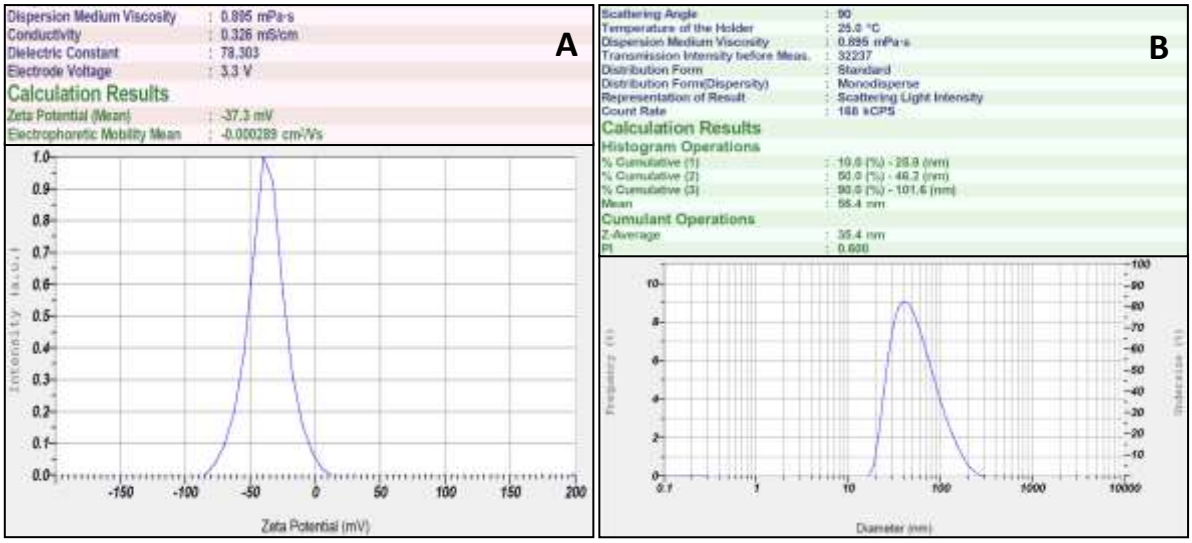

Fig. 5. (A) Zeta potential of GoLE-AgNPs: -37.3 mV, indicating stability. (B) Hydrodynamic size: 35.4 nm, PDI: 0.600, indicating monodisperse distribution

3.3. Antioxidant Activity

3.3.1 TPC and TFC of GoLE-AgNPs

The total polyphenolic content of GoLE-AgNPs synthesized from hydroacetonic leaf extract was calculated using the gallic acid equivalent (GAE) for TPC and quercetin equivalent (QE) for TFC. The TPC of GoLE-AgNPs was found to be 109.95 ± 0.311 mg GAE/100 mL at 200 µg/mL concentration with a significant R^2 value of 0.9652 (Figure 6A). The TFC of GoLE-AgNPs was found to be 34.236 ± 0.101 µg QE/mL at 200 µg/ml concentration with a significant R^2 value of 0.9918 (Figure 6B). Polyphenolics like phenolics and flavonoids chiefly act as antioxidants, capping and reducing agents that stabilize the synthesized AgNPs [30].

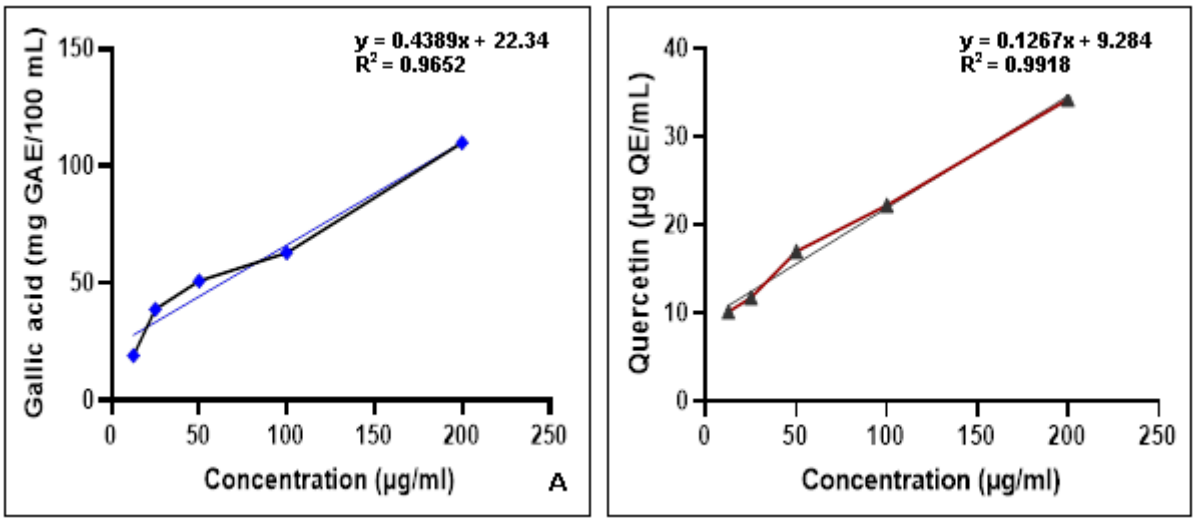

Fig. 6. (A) Total phenolic content and (B) Total flavonoid content of GoLE-AgNPs

3.3.2 DPPH radical scavenging capacity

The GoLE-AgNPs showed an effective antioxidant capacity because the phytochemicals capped on the surface of synthesized AgNPs act as effective antioxidant agents [31]. In a dose-dependent manner, GoLE-AgNPs at higher concentrations exhibited an effective percentage of inhibition of 97.39 ± 0.009 and standard ascorbic acid inhibited 93.74 ± 0.067% at 200 µg/mL concentration. The IC_{50} value of GoLE-AgNPs was 46.55 µg/ml and the standard was 35.39 µg/ml (Figure 7) (Table 1).

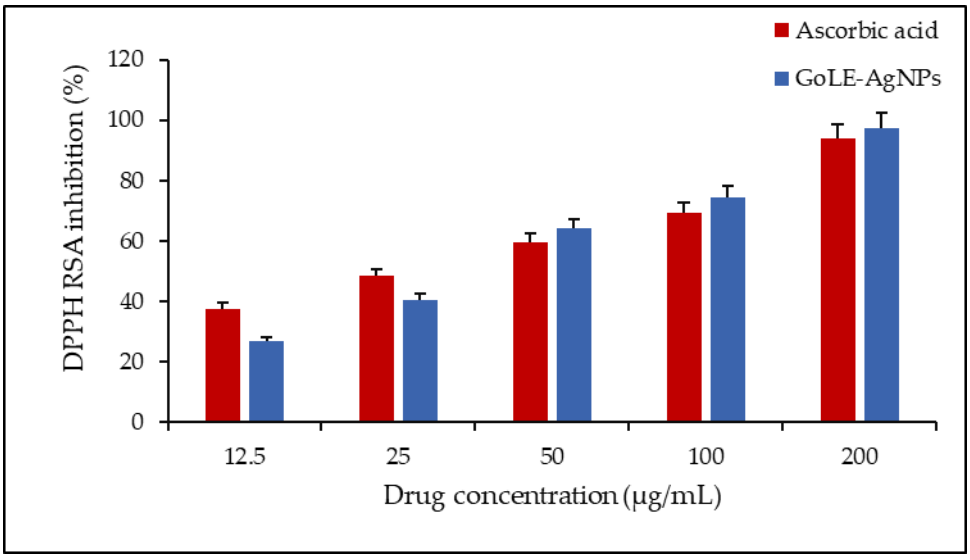

Fig. 7. DPPH radical scavenging activity of GoLE-AgNPs compared with standard ascorbic acid

Table 1
DPPH radical scavenging capacity of GoLE-AgNPs with IC_{50} concentration

Concentration (µg/ml)	Percentage inhibition (%)	
	Ascorbic acid	GoLE-AgNPs
12.5	37.53 ± 0.026	26.75 ± 0.009
25	48.30 ± 0.057	40.35 ± 0.009
50	59.52 ± 0.073	64.12 ± 0.007
100	69.09 ± 0.018	74.56 ± 0.014
200	93.74 ± 0.067	97.39 ± 0.009
IC50	35.39	46.55

Data expressed as mean ± standard deviation (n = 3)

3.4. Anticancer Activity

3.4.1 Cell viability of GoLE-AgNPs against SH-SY5Y cells

The anticancer activity of GoLE-AgNPs against cancer cell lines was investigated using MTT cell viability assay at 12.5-200 µg/ml concentrations. The results showed that cell viability decreased with increasing concentration of GoLE-AgNPs after 24 hours of treatment. The cell viability showed 24.05 ± 0.029% in the test group and 49.19 ± 0.022% in the positive control at 200 µg/ml concentration (Figure 8). Compared to standard camptothecin, the synthesized GoLE-AgNPs showed effective cell viability against SH-SY5Y cancer cell lines because the capping of potential phytoconstituents on the surface of nanoparticles enriched the cytotoxicity against the cancer cells [32]. Compared to a standard drug (195.26 µg/ml), the synthesized AgNPs showed an effective IC_{50} concentration of 130.89 µg/ml (Table 2). Due to the effective anticancer activity of silver nanoparticles crucial morphological changes like cell shrinkage and membrane blabbing were observed (Figure 9).

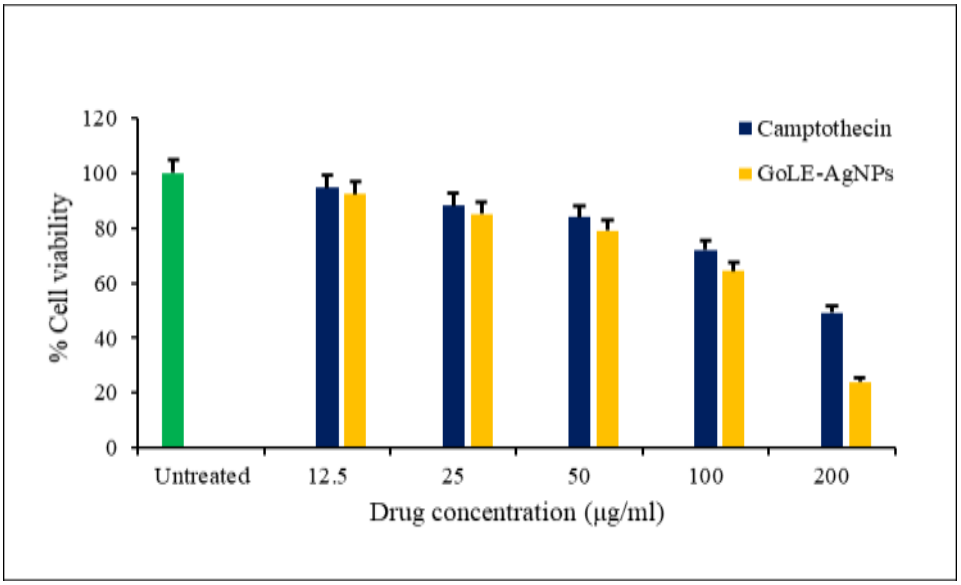

Fig. 8. Cell viability of Camptothecin and GoLE-AgNPs against SH-SY5Y cells after 24 hours of treatment

Table 2
IC_{50} concentrations of standard drug and test group in µg/mL

Cell line	Camptothecin	GoLE-AgNPs
SH-SY5Y	195.26	130.89

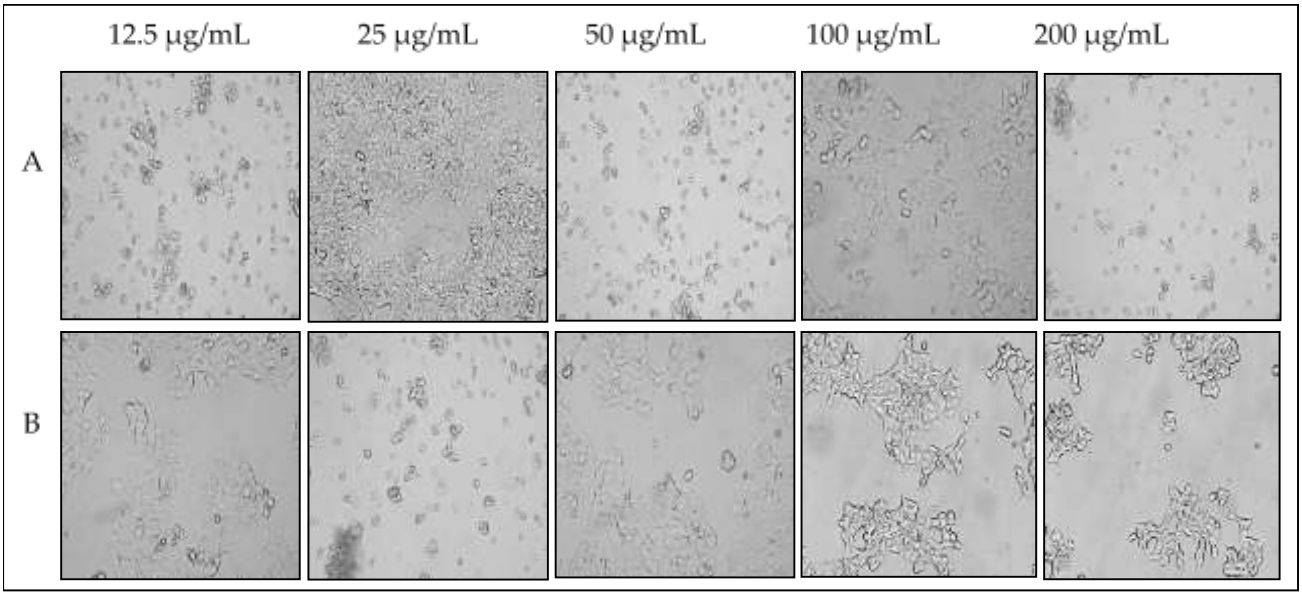

Fig. 9. Microscopic images of cell viability assay on SH-SY5Y cell lines at 12.5-200 *µg/mL concentrations* (A) SH-SY5Y cells treated with camptothecin, (B) SH-SY5Y cells treated with GoLE-AgNPs

3.4.2 GoLE-AgNPs induce apoptosis in SH-SY5Y cells

The synthesized AgNPs derived from *Guaiacum officinale* leaf extract contains therapeutic drugs like phytochemicals which efficiently induce apoptosis in Cancer cells in a dose-dependent manner [33]. Subject to IC_{50} concentrations of Camptothecin and GoLE-AgNPs for 24 hours of treatment induce apoptosis in SH-SY5Y cells. The cell populations that were necrotic, non-apoptotic, and apoptotic were all controlled by FITC Annexin V/PI staining. Figure 10A-10C and Figure 11 confirm the significant induction of necrosis (Annexin V−/PI+) (0%, 0.2% and 0.78%), late apoptosis (Annexin V+/PI+) (2.4%, 29.34% and 23%) and early apoptosis (Annexin V+/PI−) (1.23%, 23.49% and 43.13%) in SH-SY5Y cells with different treatment groups such as untreated (negative control), camptothecin (positive control), and GoBE-AgNPs (test groups) at 12.5-200 µg/mL concentrations. The rate of apoptotic cells increased from 3.63% (SH-SY5Y-Untreated) to 52.83% (SH-SY5Y-Camptothecin) and 66.13% (GoLE-AgNPs). The results validated the efficiency of GoLE-AgNPs, in inducing apoptosis in human bone marrow neuroblastoma cancer cells.

(A) (B) (C)

Fig. 10. FACS Flow cytometry examination by Annexin V FITC/PI expression in SH-SY5Y cells (A) Untreated cells of SH-SY5Y, (B) SH-SY5Y cells treated with Camptothecin, (C) SH-SY5Y cells treated with GoLE-AgNPs

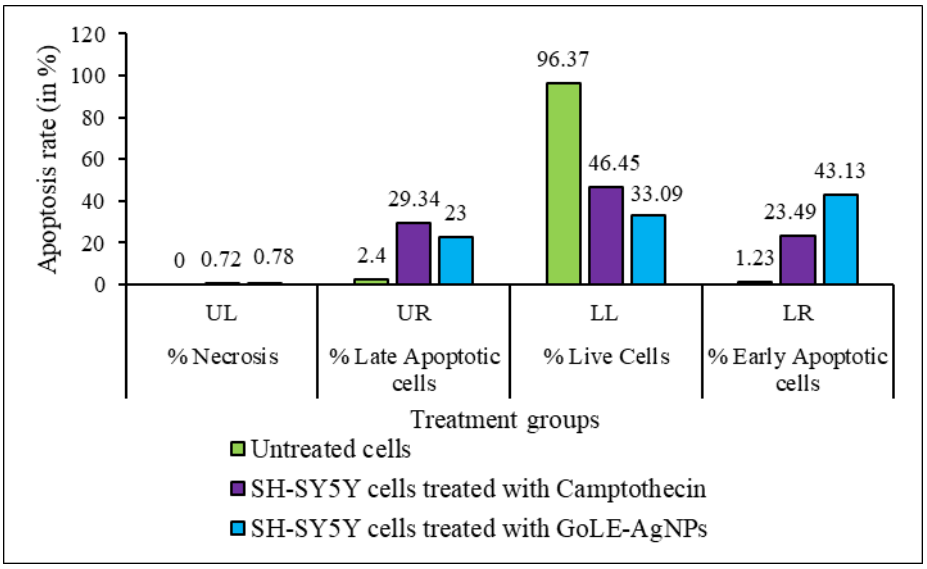

Fig. 11. Graph representing FACS Flow cytometry examination of apoptosis in treated SH-SY5Y cells. (UL- Upper left, UR- Upper right, LL- Lower left, LR- Lower right)

4. Conclusions

The invitro antioxidant and anticancer properties of silver nanoparticles synthesized from *Guaiacum officinale* leaf extract were investigated in this research work. The hydroacetonic leaf extract of *Guaiacum officinale* was prepared from an advanced ultrasonicator-assisted extraction method. Using GoLE, crystalline, phytochemically capped, small, spherical AgNPs were synthesized and analyzed by different characterization techniques. The phytochemicals play an important role in the capping, reduction, and stabilization of silver nanoparticles. The green synthesized AgNPs resulted in effective antioxidant activity and high cytotoxic to SH-SY5Y cell lines. The GoLE-AgNPs showed potential induction of apoptosis in human bone marrow neuroblastoma cancer cells. Current research evidence suggests that the green synthesized GoLE-AgNPs might be used as a potential drug for the treatment of several cancer therapies along with human bone marrow neuroblastoma cancer.

Funding

No financial support was received for this research.

Acknowledgment

The authors would like to express their sincere gratitude to – the Chairman, P. G. Department of Studies in Botany, Karnatak University, Dharwad, Karnataka, India, for the laboratory facility; to the University Scientific Instrumentation Centre (USIC), DST-PURSE Program Phase-II, Karnatak University, Dharwad, India. Sophisticated Analytical Instrument Facility (SAIF) at Dharwad, and Soniya Education Trust's College of Pharmacy, Dharwad, Karnataka, India for instrumental facilities.

References

1. Srikar, Sista Kameswara, Deen Dayal Giri, Dan Bahadur Pal, Pradeep Kumar Mishra, and Siddh Nath Upadhyay. "Green synthesis of silver nanoparticles: a review." *Green and Sustainable Chemistry* 6, no. 01 (2016): 34. https://doi.org/10.4236/gsc.2016.61004
2. Syahir, Ahmad, Sarina Sulaiman, Maizirwan Mel, Maizatulnisa Othman, and Siti Zubaidah Sulaiman. "An Overview: Analysis of ultrasonic-assisted extraction's parameters and its process." In *IOP Conference Series: Materials Science and Engineering*, vol. 778, no. 1, p. 012165. IOP Publishing, 2020. https://doi.org/10.1088/1757-899X/778/1/012165
3. Pattanayak, Sutanuka, Md Masud Rahaman Mollick, Dipanwita Maity, Sharmila Chakraborty, Sandeep Kumar Dash, Sourav Chattopadhyay, Somenath Roy, Dipankar Chattopadhyay, and Mukut Chakraborty. "Butea monosperma bark extract mediated green synthesis of silver nanoparticles: characterization and biomedical applications." *Journal of Saudi Chemical Society* 21, no. 6 (2017): 673-684. https://doi.org/10.1016/j.jscs.2015.11.004
4. Li, Peng, Xue-Mei Yin, Lu-Lu Gao, Shuai-Liang Yang, Qi Sui, Teng Gong, and En-Qing Gao. "Modulating excitation energy of luminescent metal–organic frameworks for detection of Cr (VI) in water." *ACS Applied Nano Materials* 2, no. 7 (2019): 4646-4654. https://doi.org/10.1021/acsanm.9b01088
5. Sivakumar, Allur Subramaniyan, Chandran Krishnaraj, Sunirmal Sheet, Dileep Reddy Rampa, Da Rae Kang, Shah Ahmed Belal, Abhay Kumar et al. "Interaction of silver and gold nanoparticles in mammalian cancer: as real topical bullet for wound healing—A comparative study." *In Vitro Cellular & Developmental Biology-Animal* 53 (2017): 632-645. https://doi.org/10.1007/s11626-017-0150-5
6. Skiba, Margarita I., Victoria I. Vorobyova, Alexander Pivovarov, and Natalya P. Makarshenko. "Green synthesis of silver nanoparticles in the presence of polysaccharide: optimization and characterization." *Journal of Nanomaterials* 2020 (2020): 1-10. https://doi.org/10.1155/2020/3051308
7. Vorobyova, V., G. Vasyliev, and M. Skiba. "Eco-friendly "green" synthesis of silver nanoparticles with the black currant pomace extract and its antibacterial, electrochemical, and antioxidant activity." *Applied Nanoscience* 10, no. 12 (2020): 4523-4534. https://doi.org/10.1007/s13204-020-01369-z
8. Duwiejua, M., I. J. Zeitlin, P. G. Waterman, and A. I. Gray. "Anti-inflammatory activity of Polygonum bistorta, Guaiacum officinale and Hamamelis virginiana in rats." *Journal of pharmacy and pharmacology* 46, no. 4 (1994): 286-290. https://doi.org/10.1111/j.2042-7158.1994.tb03795.x
9. Sarkar, Amrita, Poulami Datta, Asok Kumar Das, and Antony Gomes. "Anti-rheumatoid and anti-oxidant activity of homeopathic Guaiacum officinale in an animal model." *Homeopathy* 103, no. 02 (2014): 133-138. https://doi.org/10.1016/j.homp.2013.08.006
10. Niazi, Azin, Vafa Baradaran Rahimi, Nafiseh Askari, Pouria Rahmanian-Devin, and Vahid Reza Askari. "Topical treatment for the prevention and relief of nipple fissure and pain in breastfeeding women: A systematic review." *Advances in Integrative Medicine* 8, no. 4 (2021): 312-321. https://doi.org/10.1016/j.aimed.2021.07.001

11. Monclair, Tom, Garrett M. Brodeur, Peter F. Ambros, Hervé J. Brisse, Giovanni Cecchetto, Keith Holmes, Michio Kaneko et al. "The international neuroblastoma risk group (INRG) staging system: an INRG task force report." *Journal of clinical oncology* 27, no. 2 (2009): 298. https://doi.org/10.1200%2FJCO.2008.16.6876
12. Liu, Benguo, Yuxiang Ma, Yang Liu, Zhen Yang, and Liping Zhang. "Ultrasonic-assisted extraction and antioxidant activity of flavonoids from Adinandra nitida leaves." *Tropical journal of pharmaceutical research* 12, no. 6 (2013): 1045-1051. https://doi.org/10.4314/tjpr.v12i6.27
13. Pandhari, Ramachandra Mohan Rao, and Tarikere Chandrashekharappa Taranath. "In-vitro Antioxidant Activity and Flow Cytometric Analysis of Simarouba glauca DC Bark Extract Induced Apoptosis in Triple Negative Breast Cancer Cells." *Asian Pacific Journal of Cancer Prevention* 25, no. 1 (2024): 201-210. https://doi.org/10.31557/APJCP.2024.25.1.201
14. Bankalgi, Sanjeevkumar C., Ramesh L. Londonkar, Umesh Madire, and NK Asha Tukappa. "Biosynthesis, characterization and antibacterial effect of phenolics-coated silver nanoparticles using Cassia javanica L." *Journal of Cluster Science* 27 (2016): 1485-1497. https://doi.org/10.1007/s10876-016-1016-9
15. Chandra, Suman, Shabana Khan, Bharathi Avula, Hemant Lata, Min Hye Yang, Mahmoud A. ElSohly, and Ikhlas A. Khan. "Assessment of total phenolic and flavonoid content, antioxidant properties, and yield of aeroponically and conventionally grown leafy vegetables and fruit crops: A comparative study." *Evidence-based complementary and alternative medicine* 2014 (2014). https://doi.org/10.1155/2014/253875
16. Reddy, N. V., Huizhen Li, Tianyu Hou, M. S. Bethu, Zhiqing Ren, and Zhijun Zhang. "Phytosynthesis of silver nanoparticles using Perilla frutescens leaf extract: characterization and evaluation of antibacterial, antioxidant, and anticancer activities." *International journal of nanomedicine* (2021): 15-29. https://doi.org/10.2147/IJN.S265003
17. Chua, Lee Suan, Cher Haan Lau, Chee Yung Chew, and Dawood Ali Salim Dawood. "Solvent fractionation and acetone precipitation for crude saponins from Eurycoma longifolia extract." *Molecules* 24, no. 7 (2019): 1416. https://doi.org/10.3390/molecules24071416
18. Koduru, Srinivas, D. S. Grierson, M. Van de Venter, and A. J. Afolayan. "Anticancer activity of steroid alkaloids isolated from Solanum aculeastrum." *Pharmaceutical Biology* 45, no. 8 (2007): 613-618. https://doi.org/10.1080/13880200701538690
19. Koopman, G., C. P. Reutelingsperger, G. A. Kuijten, R. M. Keehnen, S. T. Pals, and M. H. Van Oers. "Annexin V for flow cytometric detection of phosphatidylserine expression on B cells undergoing apoptosis." (1994): 1415-1420. https://doi.org/10.1182/blood.V84.5.1415.1415
20. Hulkoti, Nasreen I., and T. C. Taranath. "Biosynthesis of nanoparticles using microbes—a review." *Colloids and surfaces B: Biointerfaces* 121 (2014): 474-483. https://doi.org/10.1016/j.colsurfb.2014.05.027
21. Punia Bangar, Sneh, Kawaljit Singh Sandhu, Alexandru Vasile Rusu, Pinderpal Kaur, Sukhvinder Singh Purewal, Maninder Kaur, Navneet Kaur, and Monica Trif. "Proso-millet-starch-based edible films: An innovative approach for food industries." *Coatings* 11, no. 10 (2021): 1167. https://doi.org/10.3390/coatings11101167
22. Mandal, Abhishek, Santhanam Sekar, N. Chandrasekaran, Amitava Mukherjee, and Thotapalli P. Sastry. "Vibrational spectroscopic investigation on interaction of sago starch capped silver nanoparticles with collagen: a comparative physicochemical study using FT-IR and FT-Raman techniques." *RSC advances* 5, no. 21 (2015): 15763-15771. http://dx.doi.org/10.1039/C4RA09694K
23. Nayak, Debasis, Sarbani Ashe, Pradipta Ranjan Rauta, Manisha Kumari, and Bismita Nayak. "Bark extract mediated green synthesis of silver nanoparticles: evaluation of antimicrobial activity and antiproliferative response against osteosarcoma." *Materials Science and Engineering: C* 58 (2016): 44-52. https://doi.org/10.1016/j.msec.2015.08.022
24. Singhal, Garima, Riju Bhavesh, Kunal Kasariya, Ashish Ranjan Sharma, and Rajendra Pal Singh. "Biosynthesis of silver nanoparticles using Ocimum sanctum (Tulsi) leaf extract and screening its antimicrobial activity." *Journal of nanoparticle Research* 13 (2011): 2981-2988. https://doi.org/10.1007/s11051-010-0193-y

25. Mehta, B. K., Meenal Chhajlani, and B. D. Shrivastava. "Green synthesis of silver nanoparticles and their characterization by XRD." In *Journal of physics: conference series*, vol. 836, no. 1, p. 012050. IOP Publishing, 2017. https://doi.org/10.1088/1742-6596/836/1/012050
26. Yu, Chen, Jingchun Tang, Xiaomei Liu, Xinwei Ren, Meinan Zhen, and Lan Wang. "Green biosynthesis of silver nanoparticles using Eriobotrya japonica (Thunb.) leaf extract for reductive catalysis." *Materials* 12, no. 1 (2019): 189. https://doi.org/10.3390/ma12010189
27. Bar, Harekrishna, Dipak Kr Bhui, Gobinda P. Sahoo, Priyanka Sarkar, Sankar P. De, and Ajay Misra. "Green synthesis of silver nanoparticles using latex of Jatropha curcas." *Colloids and surfaces A: Physicochemical and engineering aspects* 339, no. 1-3 (2009): 134-139. https://doi.org/10.1016/j.colsurfa.2009.02.008
28. Koppel, Dennis E. "Analysis of macromolecular polydispersity in intensity correlation spectroscopy: the method of cumulants." *The Journal of Chemical Physics* 57, no. 11 (1972): 4814-4820. https://doi.org/10.1063/1.1678153
29. Raval, Nidhi, Rahul Maheshwari, Dnyaneshwar Kalyane, Susanne R. Youngren-Ortiz, Mahavir B. Chougule, and Rakesh K. Tekade. "Importance of physicochemical characterization of nanoparticles in pharmaceutical product development." In *Basic fundamentals of drug delivery*, pp. 369-400. Academic Press, 2019. https://doi.org/10.1016/B978-0-12-817909-3.00010-8
30. Sulaiman, C. T., and Indira Balachandran. "Total phenolics and total flavonoids in selected Indian medicinal plants." *Indian journal of pharmaceutical sciences* 74, no. 3 (2012): 258. https://doi.org/10.4103%2F0250-474X.106069
31. Bhakya, S., S. Muthukrishnan, M. Sukumaran, and M. Muthukumar. "Biogenic synthesis of silver nanoparticles and their antioxidant and antibacterial activity." *Applied Nanoscience* 6 (2016): 755-766. https://doi.org/10.1007/s13204-015-0473-z
32. Satyavani, K., S. Gurudeeban, T. Ramanathan, and T. Balasubramanian. "Biomedical potential of silver nanoparticles synthesized from calli cells of Citrullus colocynthis (L.) Schrad." *Journal of nanobiotechnology* 9 (2011): 43. https://doi.org/10.1186/1477-3155-9-43
33. Choudhari, Amit S., Pallavi C. Mandave, Manasi Deshpande, Prabhakar Ranjekar, and Om Prakash. "Phytochemicals in cancer treatment: From preclinical studies to clinical practice." *Frontiers in pharmacology* 10 (2020): 497776. https://doi.org/10.3389/fphar.2019.01614